# Unusual scarcity in the optical absorption of metallic quantum-dot nanorings described by the extended Hubbard model

Ioan Bâldea* and Lorenz S. Cederbaum
*Theoretische Chemie, Physikalisch-Chemisches Institut, Universität Heidelberg, Heidelberg 69120, Germany*
(Received 17 January 2008; revised manuscript received 31 March 2008; published 29 April 2008; corrected 27 May 2008)

We report results of a systematic analysis of optical absorption in finite metallic quantum-dot nanorings containing a variable number of electrons described by the extended Hubbard model. Despite the very strong electron correlations, the number of significant spectral lines is astonishingly small, and the optical spectra can still be rationalized within a simple framework relying upon the single-particle picture. The main effect of correlations is to split the optical transitions that are degenerate within the single-particle description and to give rise to numerous avoided crossings (anticrossings). Unusually, the latter often involve more than two states. For closed-shell systems, the optical spectrum is practically monochromatic. We also present results of an approximate scheme, based on the Landau idea to describe low excitations in an interacting electron system. It consists of diagonalizing the Hamiltonian in the configuration interaction truncated to include dressed particle-hole excitations derived from the exact ground state. This method provides a good description of the overall optical absorption, including that of the diabatic state corresponding to the bright transition at avoided crossings. The scarcity in the optical spectra reported here points toward a hidden dynamical quasisymmetry in the optical absorption of finite nanorings described within the extended Hubbard model, generalizing thereby our recent finding [I. Bâldea and L. S. Cederbaum, Phys. Rev. B **75**, 125323 (2007)]. In addition, we report a qualitative difference between the optical gap and the charge gap occurring at quarter filling.

DOI: 10.1103/PhysRevB.77.165339 PACS number(s): 78.67.Hc, 73.21.La, 73.63.Kv, 85.35.Be

## I. INTRODUCTION

Advances in nanotechnologies attempt to bridge the gap between molecules and solids, by assembling metallic quantum dots (QDs) in extended regular nanostructures.[1–8] Individual QDs resemble artificial atoms.[9] With the motion confined within a few nanometers, electrons occupy quantized levels, well separated energetically, similar to atomic orbitals (AOs) in ordinary atoms. Assembled in dense nanostructures, QDs are coupled via electron tunneling and mutual capacity effects. The former, which results from overlapped wave functions between adjacent dots, causes delocalization of a few "valence" (or $\pi$) electrons over the whole nanostructure. Unlike those of ordinary atoms, molecules, or solids, the properties of QD nanostructures—and this is their salient feature—are easily tunable in wide ranges by varying parameters easily controlled experimentally, such as dot diameter ($2R$), interdot spacing ($D$),[1–8] or gate voltages.[10]

The tunable properties make assembled QDs ideal systems for studying (strong) electron correlation effects. In this paper, we shall focus our attention on the optical absorption of QD nanorings described by means of the extended Hubbard model. From extensive studies of molecular and solid-state physics,[11] it is well known that this property is very sensitive to electron correlations.

Perhaps the most important issue of the present paper is that, despite of strong correlations, optical absorption spectra of the nanorings are astonishingly scarce. This statement is based on exact numerical diagonalization results for finite rings. This finding represents a generalization of our recent result on the near monochromaticity of the optical spectrum in half-filled nanorings.[12]

The remaining part of the paper is organized in the following manner: The model of the theoretical study of QD nanorings is presented in Sec. II. By analyzing the electron correlations in Sec. III, we show that it is possible to continuously drive the investigated systems from a weak to a strong correlation regime. General aspects related to the property on which we mainly focus, the optical absorption, are discussed in Sec. IV. Next, we discuss in detail optical absorption for nanorings with a variable number of electrons. Because of qualitative differences, optical absorption for closed and open shells is analyzed in separate sections, Secs. V and VI, respectively. In Sec. V, we present the results both for the case of half-filling (Sec. V A) and away from half-filling (Sec. V B). Then, in Sec. VI, we consider in detail various cases of open-shell nanorings (Secs. VI A–VI D). In Sec. VII we show that the exact results can be accurately reproduced by means of an approximate method, considerably less demanding than exact numerical diagonalization. In Sec. VIII, we comparatively analyze two related but distinct quantities, the optical gap and the charge gap. Finally, Sec. IX makes the object of some discussions and conclusions.

## II. MODEL

Isolated QDs are characterized by the on-site Coulomb repulsion energy $U$ (related to self-elastance or Coulomb blockade) and the energy of valence electrons $\epsilon$. These quantities can be controlled by varying the dot diameter $2R$. Assembled in nanorings, QDs are coupled both by electron tunneling (resonance integral $t_0$) and by Coulomb interaction $V$ (related to the mutual elastance). These parameters can be tuned by adjusting the interdot separation $D$. In addition, the number of electrons can easily be changed within wide ranges by varying the voltage of a gate electrode, which is placed on the top of the electron gas.[10]

 

To account for the physical aspects mentioned above, following, e.g., Refs. 12–15, we shall model a nanoring with $N$ QDs contains $N_e$ valence electrons (arbitrary-filling case) by means of the one-band extended Hubbard (in chemists' nomenclature, Pariser–Parr–Pople) Hamiltonian,

$$H = -t_0 \sum_{l=1}^{N} \sum_{\sigma=\uparrow,\downarrow} (a_{l,\sigma}^{\dagger} a_{l+1,\sigma} + a_{l+1,\sigma}^{\dagger} a_{l,\sigma}) + \sum_{l=1}^{N} (U \hat{n}_{l,\uparrow} \hat{n}_{l,\downarrow} + V \hat{n}_l \hat{n}_{l+1}), \quad (1)$$

where $a_{l,\sigma}$ ($a_{l,\sigma}^{\dagger}$) denote the creation (annihilation) operators for electrons of spin $\sigma$ on the $l$th QD, $\hat{n}_{l,\sigma} \equiv a_{l,\sigma}^{\dagger} a_{l,\sigma}$, and $\hat{n}_l \equiv \hat{n}_{l,\uparrow} + \hat{n}_{l,\downarrow}$,

In Eq. (1), we have assumed an ideal situation, wherein the model parameters are site independent. This can be considered a reasonable first-order approximation in view of the narrow size distributions (~2–5%) achieved in the arrays of Ag QDs assembled by Heath's group.[1–8] As discussed in Ref. 12, such a weak disorder do not have a dramatic impact on optical absorption. The analysis of the model parameters $t_0$, $U$, and $V$ has been presented earlier in literature. The hopping integral $t_0$ was determined in Ref. 16 by fitting the second harmonic response experimentally measured[1] for an array of Ag QDs of size $2R=2.6$ nm and used in a series of subsequent studies.[13,17–21] $U$ was determined by scanning electron microscopy experiments ($U \sim 0.3-0.34$ eV for $2R=2.6$ nm),[5] in agreement with the spherical model, and subsequently employed in interpreting later experiments by Heath and co-workers.[6–8] The $d$-dependent self-elastance and mutual elastance (and thence $U$ and $V$) have been obtained by considering electrostatically coupled QDs.[22] The restriction to a single AO per QD (one-band extended Hubbard model) in Eq. (1) is justified by the large energy separation of the levels in a small spherical box.

Concerning the method, we note that the exact numerical results reported in this paper have been obtained by means of the Lanczos algorithm. As discussed elsewhere,[15,23,24] by running the Lanczos procedure three times, we are able to directly compute the frequencies and the intensities of the spectral lines. In the method more familiar in condensed matter physics,[25–27] by using the continued fraction algorithm, only convoluted spectra can be calculated.

## III. ELECTRON CORRELATIONS

The Langmuir technique that is experimentally employed[1–8] enables a broad tuning of the hopping integral $t_0 \propto \exp(-5.5d)$ by varying the interdot spacing $d$ within the range $1.1 \lesssim d \lesssim 1.85$ of experimental interest. In this way, broad ranges of the parameter space $(U/t_0, V/t_0)$ of the extended Hubbard model can be explored (see Fig. 1). Therefore, it is possible to practically switch continuously from the weak correlation regime to the strong correlation regime. In the former limit, the QDs are close enough to each other ($d \gtrsim 1$) and efficient tunneling yields electrons that are completely delocalized over the whole nanoring. Correlations are practically absent and the single-particle description in terms of molecular orbitals (MOs) holds true. Up to, say, $d \lesssim 1.3$, one can clearly distinguish between (almost) fully occupied

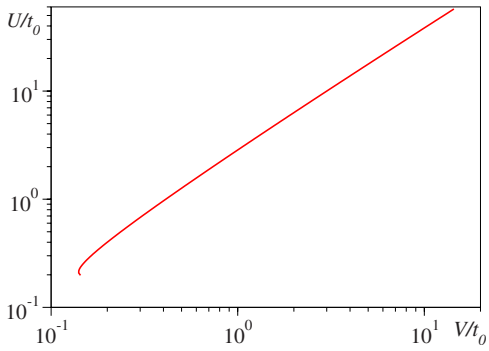


FIG. 1. (Color online) Curve in the $(U/t_0, V/t_0)$ plane accessible by varying the interdot spacing in the range $1 < D/(2R) < 2$ in assemblies of QDs of silver, showing that broad parameter ranges can be explored. Notice the logarithmic scale on both axes.

MOs with occupancy $n_p \equiv \langle G | c_{p,\sigma}^{\dagger} c_{p,\sigma} | G \rangle \approx 1$ inside the Fermi sea, $|p| < p_F$, and (almost) empty MOs, $n_p \approx 0$, outside the Fermi sea, $|p| > p_F$. Here, $c_{p,\sigma} = 1/\sqrt{N} \Sigma_l a_{l,\sigma} \exp(-2\pi p l i/N)$ denote MO (Bloch) operators, $p_F$ is the Fermi momentum and $|G\rangle$ the exact ground state. For illustration, see Fig. 2 for the half-filling case (six electrons over six QDs and ten electrons over ten QDs), where $p_F = \pi/2$. Because of the fast, exponential fall-off of the hopping integral, the MO picture rapidly worsens and finally breaks down with increasing $d$. One arrives at a situation wherein one cannot distinguish between occupied and unoccupied orbitals any longer. Then, for half-filling, all orbitals become democratically occupied $n_{p,\sigma} \approx 0.5$ (see Fig. 2). Electron tunneling becomes negligible, and the lowest (ground state) energy is reached by localized electrons that avoid double occupancy on the same dot.

To end Sec. III, we note that in Fig. 2 the values of the momentum distribution $n_p$ for six electrons over six QDs and ten electrons over ten QDs build smooth curves. This behavior, which was also encountered in other cases, is related to the fact that rings with $N = N_e = 4\kappa + 2$ (with integer $\kappa$) belong to the class of the so-called Hückel systems (see, e.g., Refs. 28–30).

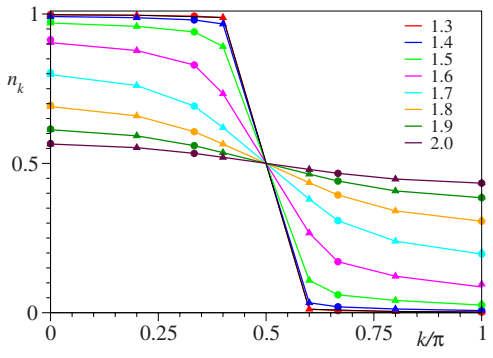


FIG. 2. (Color online) Momentum distribution in the ground state of six (circles) and ten (triangles) half-filled QDs for several values of interdot spacing $d$ given in the legend. The values of $d$ that increase downward for $k/\pi < 0.5$ are given in the legend. The lines are guides for the eyes (Ref. 31).

## IV. OPTICAL ABSORPTION

The property of our main interest here is the optical absorption in the ground state. Optical absorption provides information on the dipole allowed transitions from a reference state; at sufficiently low temperatures $T \gtrsim 0$, this is usually the ground state. The quantities of interest are the excitation energies $\varepsilon_\lambda - \varepsilon_G$ and the matrix elements of the electric dipole $\boldsymbol{\mu}$, which enter the absorption coefficient in the ground state $|G\rangle$. In the ring plane specified by the unit vectors $(\hat{\mathbf{x}}, \hat{\mathbf{y}})$, the electric dipole operator is expressed by

$$\boldsymbol{\mu} = -|e|\rho \sum_l \hat{n}_l [\hat{\mathbf{x}} \cos(2\pi l/N) + \hat{\mathbf{y}} \sin(2\pi l/N)], \tag{2}$$

where $e$ and $\rho = D/2 \sin(\pi/N)$ denote the elementary charge and ring radius, respectively.

For later considerations, the expression of the dipole momentum in terms of MO (Bloch) operators $c_{p,\sigma}$ is also useful,

$$\mu_x = -|e|\rho/2 \sum_{p,\sigma} (c^\dagger_{p+1,\sigma} c_{p,\sigma} + c^\dagger_{p,\sigma} c_{p+1,\sigma}),$$

$$\mu_y = i|e|\rho/2 \sum_{p,\sigma} (c^\dagger_{p+1,\sigma} c_{p,\sigma} - c^\dagger_{p,\sigma} c_{p+1,\sigma}). \tag{3}$$

The absorption coefficient of a nanoring shined by a laser field linearly polarized along $j$ direction $(j = x, y)$ of the ring plane can be written as

$$\alpha_j(\omega) = \rho^{-2} \omega \sum_\gamma \sum_{\lambda \in \Gamma_\gamma} |\langle \Psi_\lambda | \mu_j | G \rangle|^2 \delta(\omega - \varepsilon_\lambda + \varepsilon_G). \tag{4}$$

Because of symmetry, $\alpha_x(\omega) = \alpha_y(\omega)$, and hereafter we shall drop the subscript. Within the point group $D_{Nh}$ relevant for nanorings with $N$ QDs, the components $(\mu_x, \mu_y)$ of the electric dipole operator $\boldsymbol{\mu}$ transform according to the two-dimensional irreducible representation $E_{1u}$, and therefore only eigenstates with $\Gamma_\gamma$ symmetry satisfying

$$\Gamma_\gamma \otimes E_{1u} \otimes \Gamma_G \supset A_{1g}, \tag{5}$$

which contribute to optical absorption. Here, $\Gamma_G$ denotes the ground state symmetry.

For the considerations on optical absorption in Secs. V and IX, it is important to note the occurrence of the consecutive indices ($p$ and $p+1$) in Eq. (3). This implies that only transitions between *adjacent* MOs can contribute to optical absorption. Below, we shall present results on optical absorption for nanorings consisting of six and ten QDs. Therefore, to facilitate understanding, it is useful to note that in the former case the MOs ordered by increasing energy are a nondegenerate $a_{1g}$ MO ($p=0$), two degenerate $e_{1u}$ ($p=\pm 1$) and $e_{2g}$ ($p=\pm 2$), and a nondegenerate $b_{1u}$ MO ($p=3$). For rings with ten QDs, ordered by increasing energy, the ten MOs are a nondegenerate $a_{1g}$ MO ($p=0$), two degenerate $e_{1u}$ ($p=\pm 1$), $e_{2g}$ ($p=\pm 2$), $e_{3u}$ ($p=\pm 3$), $e_{4g}$ ($p=\pm 4$) MOs, and a nondegenerate $b_{1u}$ MO ($p=5$).

Below, we shall examine nanorings with a variable number of electrons $N_e$. Because of the particle-hole symmetry of model (1), one can restrict oneself to values $N_e \leq N$. The cases of closed and open shells will be separately discussed. In the analysis below, one should keep in mind that both the total spin and the total spin projection are conserved in optical absorption.

Concerning the effect of electron correlations, it is worth remembering that in view of space symmetry, free (Bloch) electron states exactly satisfy the Hartree–Fock equations (see, e.g., Ref. 32). As a consequence, all absorption frequencies scale as the hopping integral $t_0$ within the MO approximation. Therefore, in the figures presented below with logarithmic scale on ordinates, the corresponding curves would be straight lines tangent to the exact curves for small $d$ because electron correlations are very weak for $d \gtrsim 1$. In the figures, we shall not present these rather trivial lines of the single-particle approximation, but one should keep in mind that deviations from the linearity of the exact curves measure the effect of electron correlations. Apart from exact results, we shall present instead approximate results obtained by diagonalizing the exact Hamiltonian on the basis of the particle-hole excited states of the MO approximation. Accidentally, because of the aforementioned particularity of the Hartree–Fock equations, this approximation actually amounts to the first-order perturbation theory. Therefore, the label p.t. will be used for the curves computed within this approximation. This first-order perturbation theory is applied for nondegenerate states in the cases discussed in Sec. V and for degenerate states for those in Sec. VI.

In all of the cases presented in Secs. V and VI, we find a small number of optical transitions with significant spectral intensities, which are astonishingly small considering that the electron correlations are strong and very numerous transitions are allowed by spin conservation and spatial symmetry. Other contributions from other allowed transitions also exist but are not shown because they are substantially smaller. In this respect, the situation is similar to the half-filling case recently discussed in Ref. 12.

In Secs. V–VIII, we shall present results on absorption frequencies and intensities for the relevant optical transitions. Because the former can be directly compared to experiments, we express them in electronvolts. Since only *convoluted* theoretical spectra are of interest to experimentalists, less attention will be paid to the units of the absorption coefficient $(\varepsilon_\lambda - \varepsilon_G)|\langle \Psi_\lambda | \mu_j | G \rangle|^2$ [cf. Eq. (4)], and we write generically arb. units. To be specific, this "arbitrary unit" (the *same* in all figures) is electronvolt times squared elementary charge.

## V. CASE OF CLOSED SHELLS

For closed-shell systems, within the MO picture the lower-energy MOs are fully occupied up to the highest occupied molecular orbital (HOMO), while the higher-energy MOs, starting from the lowest unoccupied molecular orbital (LUMO), are completely empty in the ground state. Only a single transition is optically allowed, which amounts to the excitation of an electron from the HOMO into the LUMO, and this requires an excitation energy called the HOMO-LUMO gap. Within the MO picture, all closed-shell systems

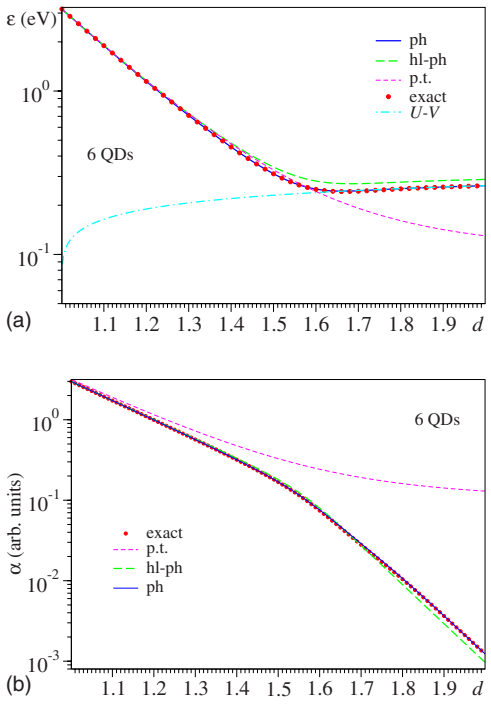


FIG. 3. (Color online) Absorption frequency and intensity of the relevant spectral line for six-QD nanorings at half-filling. For small $d$ the exact results (represented by points) are well approximated by those of the perturbation theory (p.t.) (see Sec. IV), whereas for large $d$ the absorption frequency approaches the asymptotical limit $U$-$V$ (see main text). Concerning the curves denoted by *hl-ph* and *ph*, see Sec. VII.

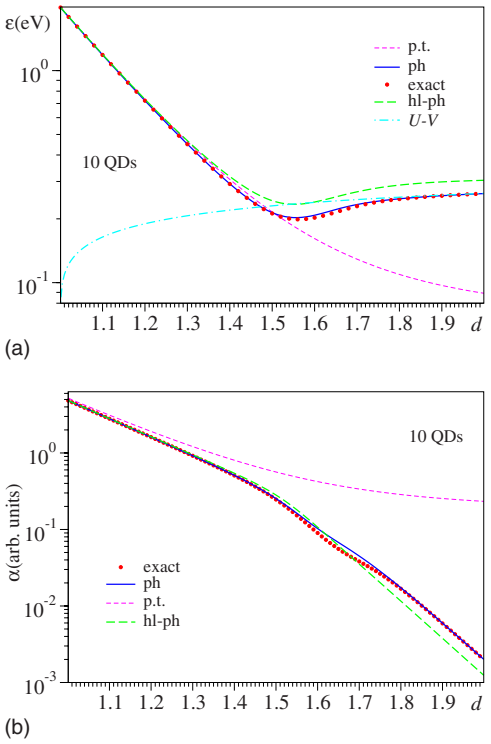


FIG. 4. (Color online) Absorption frequency and intensity of the relevant spectral line for ten-QD nanorings at half-filling. The meaning of the various curves is indicated in the legends and explained in the caption of Fig. 3.

behave qualitatively similar. In the presence of electron correlations, however, as shown below, the case of half-filling represents a special case, with a behavior qualitatively different from other closed-shell cases away from half-filling.

### A. Case of half-filling

Because the case of half-filling was already presented in our earlier work,[12] here, we restrict ourselves to only a few aspects relevant for the present context. At half-filling, in agreement with the MO picture, we always numerically found that the ground state $|G\rangle$ is a $^1A_{1g}$ singlet for all $d$'s. Therefore, in principle all excited singlet $^1E_{1u}$ states could contribute to optical absorption [Eq. (4)]. For six-QD nanorings, out of 175 singlet states, there are 54 states of $^1E_{1u}$ symmetry.[33] For ten-QD nanorings, there are 19404 singlet states, and thousands thereof possess $E_{1u}$ symmetry. Therefore, in view of the strong correlations (cf. Sec. III), one would expect a multitude of optical transitions or, rephrasing, a rich optical spectrum. However, and this was the astonishing result reported in Ref. 12, the contrary is true: even in the presence of strong electron correlations, the spectrum remains practically monochromatic, a fact we attributed to a hidden dynamical quasisymmetry.

Results for the absorption frequency (which is also the optical gap here) and the intensity of the single relevant spectral line are shown in Figs. 3 and 4. By inspecting the exact results on the absorption frequency [points in Figs. 3(a) and 4(a)], one can easily identify the weak and strong correlation regimes for smaller and larger interdot spacings $d$, respectively. In the former regime, the optical gap, which is basically a HOMO-LUMO gap (or band gap) $\approx 2t_0 \sin(\pi/N)$, is in good agreement with the MO description (the curve is almost linear). It decreases with increasing $N$ and exponentially falls off, similar to the hopping integral $t_0$ (note the logarithmic scale on the ordinate). In the latter regime, it is reminiscent of the *finite* Mott–Hubbard gap. This represents the gap of charge excitations, which is known from the study of the infinite restricted Hubbard model (i.e., with $V=0$) to be nonvanishing only at half-filling.[34,35] (See also Sec. VIII.) Loosely speaking, the Mott–Hubbard gap is the energy necessary to create a doubly occupied site. In the limit of vanishing hopping ($t_0 \to 0$), the double occupancy is avoided in the ground state because it costs a large energy ($U$). To create a charge excitation requires an energy $U$-$V$ (for $U > V$), and one can see that this is just the limit approached by the exact optical gap. Noteworthy is that in this case, of large $d$, the optical gap tends to a limit ($U$-$V$) that is independent of $N$. This fact is understandable because for large $d$ the dots are practically no longer coupled by tunneling. Figures 3(a) and 4(a) suggest a practical criterion to reasonably define a critical point $d_0$ for the crossover between weak and strong correlation regimes: equate the asymptotic limit ($U$-$V$) with the single-particle gap.

From the fact that the spectrum is practically monochromatic, like within the single-particle picture, one may think that correlation effects on optical absorption are altogether

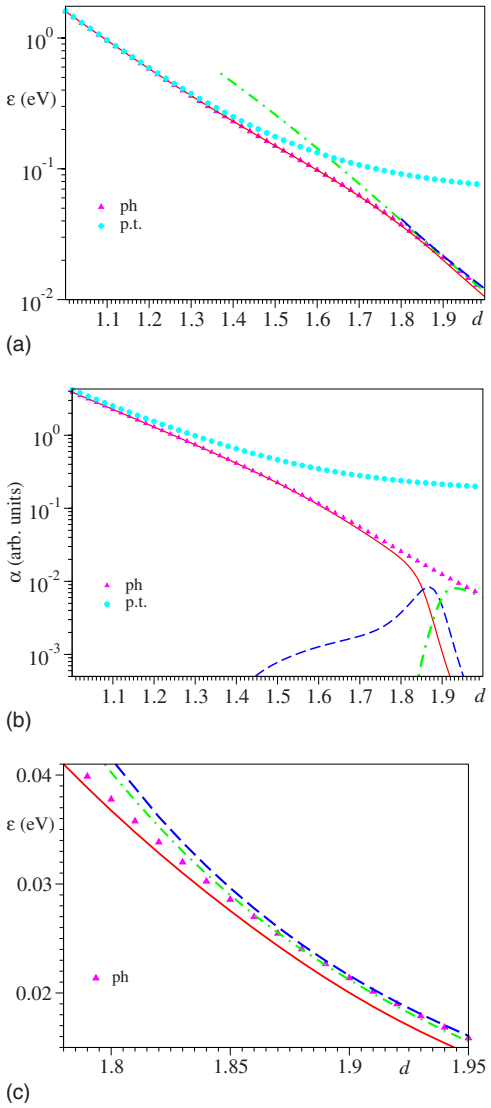


FIG. 5. (Color online) [(a) and (c)] Energies and (b) spectral intensities of optical absorption for six electrons on ten QDs in the ground ($^1A_{1g}$) state. Only three excited $E_{1u}$ states are important, which are shown by the solid, dashed, and dashed-dotted lines. Note that except around $d \approx 1.87$, where an avoided crossing involving all these three states occurs, practically only one optical transition possesses a significant intensity. Because of the small energy splitting at the avoided crossing, the measured spectrum is practically monochromatic and has a smoothly varying intensity in the whole $d$ range, which is well approximated by the results of the *ph* approximation (see Sec. VII). In (c), the *ph* curve for energy has been shifted downward by 0.7 meV. For small $d$, the exact results are well approximated by those of the perturbation theory (p.t.) (see Sec. IV).

ineffective. However, the opposite is true: the results (*p.t.*) of the perturbation theory, which are also depicted in Figs. 3 and 4, are close to the exact ones in the weak correlation regimes but substantially depart from the latter in the strong correlation regime.

In Sec. V A, we do not analyze all of the curves in Figs. 3 and 4, but postpone their analysis until Sec. VII. Below, we similarly proceed with Figs. 5–7 and 9.

### B. Closed shells away from half-filling: Nanorings with six electrons on ten quantum dots

Let us now consider a closed-shell nanoring away from half-filling. For illustration, we present results on optical absorption for a ten QD nanoring with six valence electrons in Fig. 5. Three optical transitions play an important role in this case, which are represented by the solid, dashed, and dotted lines in Fig. 5.

Very interesting is the region around $d=d_c \approx 1.87$, where a phenomenon termed "avoided crossing" by molecular physicists and "anticrossing" by solid-state physicists occurs. What makes the difference from other cases of avoided crossings from molecular and solid-state physics on which we are aware is the fact that *three* and not only two states are involved in the case depicted in Fig. 5. As shown in Sec. VI, the participation of more than two states to avoided crossings in QD nanorings is the rule rather than the exception.

Note that the optical transition is intense only to one of the $E_{1u}$ states, namely, to that which is expected in the MO picture (HOMO-LUMO transition) except around the avoided crossing. Because of the small energy differences of the three states around $d \approx 1.87$, one cannot separately measure the three intensities represented by the solid, dashed, and dotted lines in Fig. 5, but rather their sum. This means that in practice, the absorption spectrum is also practically monochromatic, in accord with what one expects within the MO picture, and similar to the half-filling case (Sec. V A and Ref. 12).

However, there is an important difference from the latter case. While the optical gap remains finite at half-filling, it exponentially decreases with $d$ in the present case. We found the same behavior for other cases of closed shells away from half-filling numerically studied. Again, this is a counterpart to the behavior known from the infinite *restricted* Hubbard model ($V=0$), where one can distinguish two phases: a metallic phase away from half-filling and a Mott insulating phase at half-filling. The lowest excitations of the metallic phase have a gapless spectrum, while the excitations of the insulating phase have a finite gap due to on-site repulsion ($U>0$). Further details will be discussed in Sec. VIII.

## VI. CASE OF OPEN SHELLS

For open-shell systems, there exists a certain molecular orbital, which is partially occupied, lying above fully occupied orbitals and below completely empty orbitals. The absorption spectrum within the MO picture consists of two lines, which correspond to an excitation of an electron either into or from the partially occupied molecular orbital (absorption frequencies $\varepsilon_1$ and $\varepsilon_2$, respectively, $\varepsilon_1 < \varepsilon_2$). For odd electron systems, unless otherwise specified, we restrict ourselves below to the spin doublet states ($S=1/2$, $S_z=+1/2$).

### A. Cases of five electrons on six quantum dots and five electrons on ten quantum dots

The ground state is a spin doublet $^2E_{1u}$ state both for five electrons on six QDs and for five electrons on ten QDs. Both

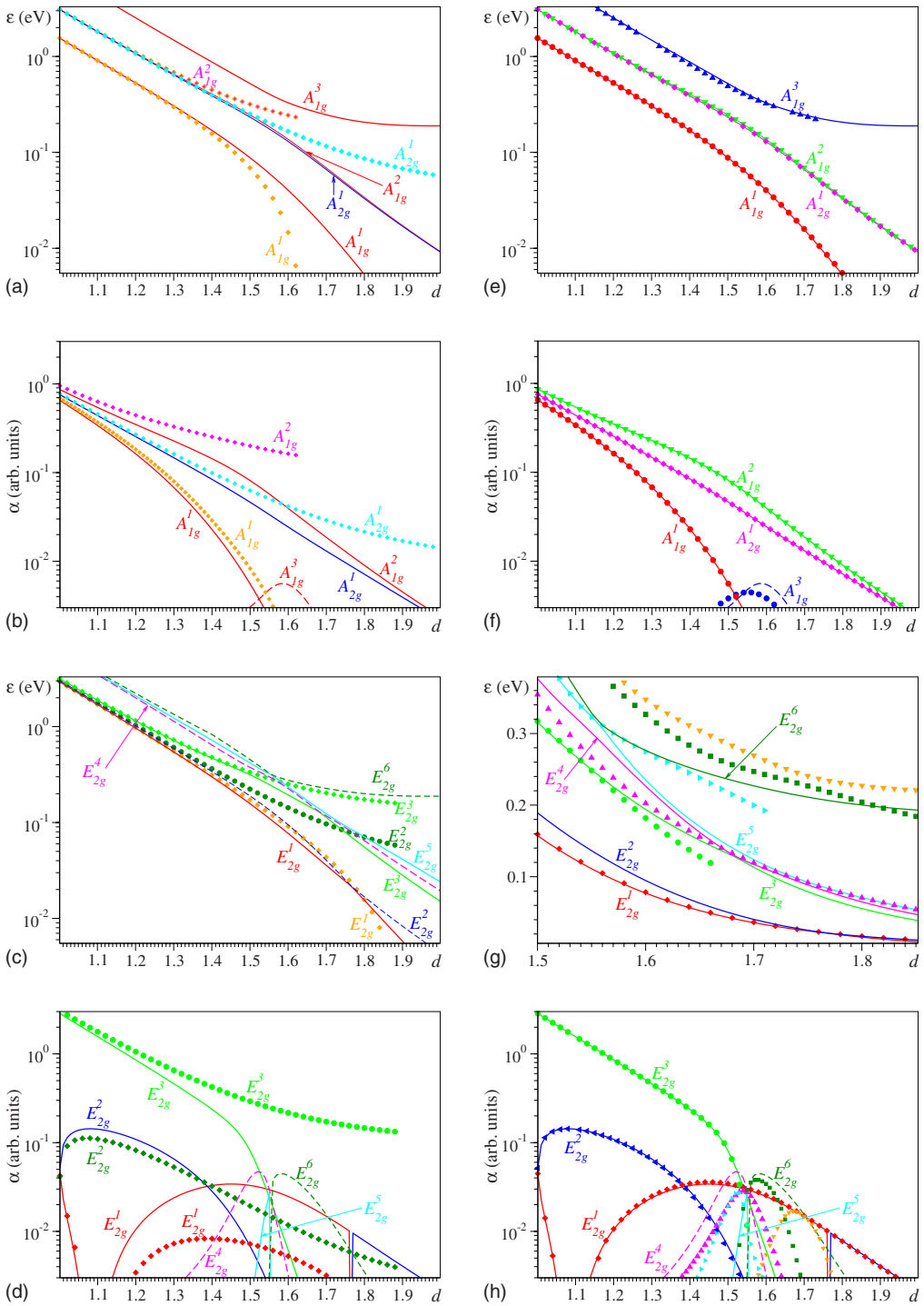


FIG. 6. (Color online) Results for optical absorption of five electrons on six QDs. The superscripts indicate the energy ordering of the excited states with significant spectral intensity. The solid lines represent the exact results. In (a)–(d), the points represent the results of perturbation theory (*p.t.*), while in (e)–(h), they are the results of the *ph* method (see Sec. VII). In (g), the diabatic *ph* curve approximating the exact energies of $E^5_{2g}$ and $E^6_{2g}$ in the regions where these two are bright (for $d \lesssim 1.56$ and $d \gtrsim 1.56$, respectively) has been shifted downward by 5.5 meV.

in the $D_{6h}$ and the $D_{10h}$ point groups, $\boldsymbol{\mu}|G\rangle \rightarrow E_{1u} \otimes E_{1u} = A_{1g} \oplus A_{2g} \oplus E_{2g}$. Therefore, only spin doublet excited states of symmetries $A_{1g}$, $A_{2g}$, and $E_{2g}$ can contribute to optical absorption. In Figs. 6 and 7, we show the spectral intensities and the absorption frequencies of the optical transitions to the aforementioned states.

As already mentioned, within the MO picture the absorption spectrum from the ground state consists of two spectral lines. The first allowed transition corresponds to the excitation of an electron from an $a_{1g}$-MO to an $e_{1u}$-MO, and this yields a (orbitally) nondegenerate excited $^2A_{1g}$ state. We shall denote this state by $A^1_{1g}$, as part of a general notation

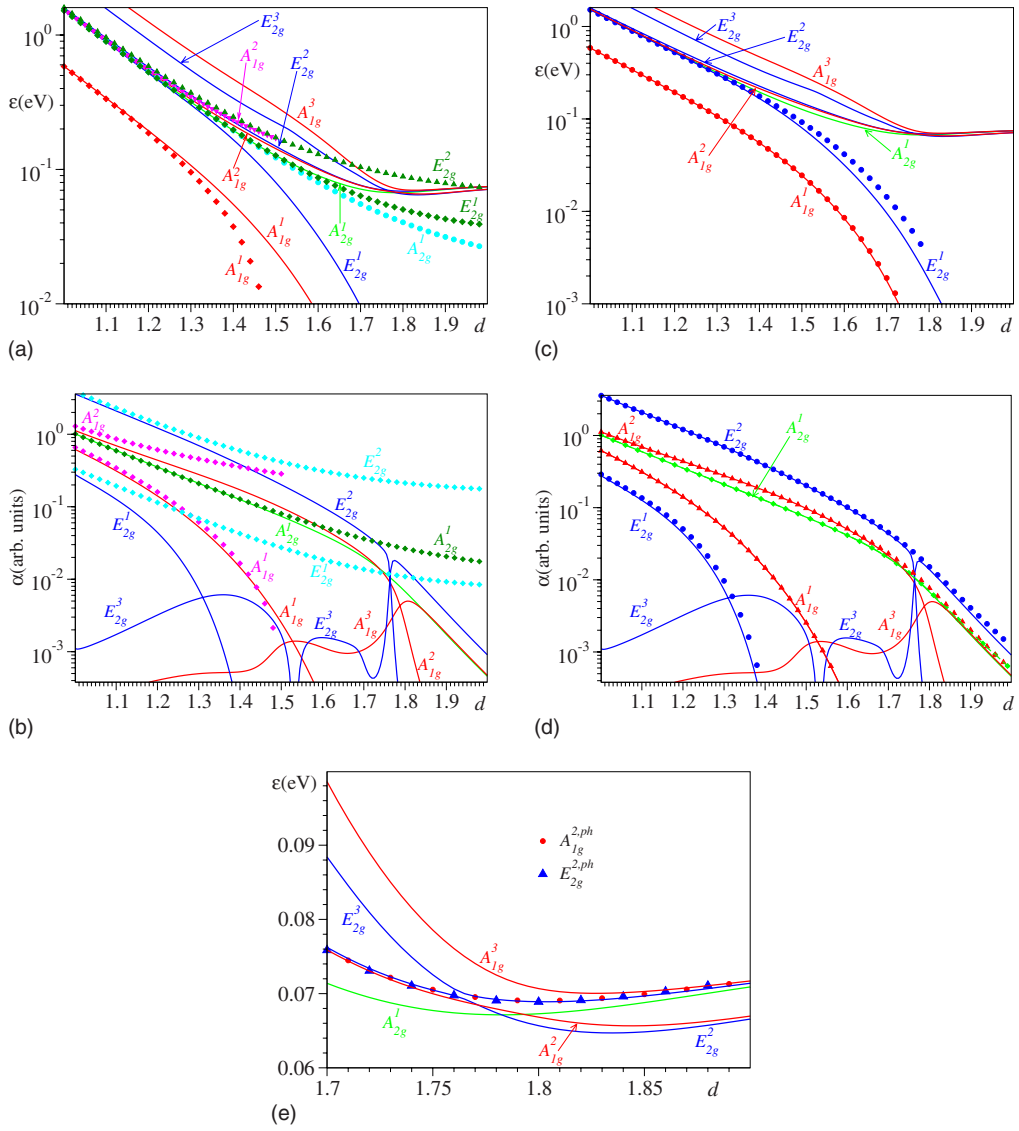


FIG. 7. (Color online) Energies and spectral intensities of optical absorption for five electrons on ten QDs in the ground ($E_{1u}$) state. The solid lines represent the exact results. The superscripts indicate the energy ordering of the excited states with a significant spectral intensity. In (a) and (b), the points are the results of the *p.t.* approximation (see Sec. IV). In (c), (d), and (e), the points represent the results of the *ph* approximation (see Sec. VII).

used throughout hereafter. Namely, we shall drop the left superscript of spin multiplicity for excited states (which is the same as in the ground state since optical transitions conserve the spin) and use (right) superscripts to label the excited states that significantly contribute to optical absorption ordered in ascending energy. For the second excitation energy, an electron is excited from an $e_{1u}$-MO to an $e_{2g}$-MO. For a fixed total spin $S=1/2$ and spin projection $S_z=+1/2$, in the case of five electrons on six QDs, this transition comprises the following group of *degenerate* excited states: one $^2A_{1g}$ state (denoted by $A_{1g}^2$), one $^2A_{2g}$ ($A_{2g}^1$), and three states $^2E_{2g}$ ($E_{2g}^1$, $E_{2g}^2$, and $E_{2g}^3$). For five electrons on ten QDs, the group of degenerate excitations comprises one $^2A_{1g}$ state ($A_{1g}^2$), one $^2A_{2g}$ ($A_{2g}^1$), two states $^2E_{2g}$ ($E_{2g}^1$ and $E_{2g}^2$), and one state $^2E_{4g}$.

At smaller $d$, the main effect of the electron correlations induced by the Hubbard terms consists of lifting this degeneracy in the above mentioned second group of optically active excitations. To illustrate this, in Figs. 6(a)–6(d), 7(a), and 7(b), we have plotted the exact curves (solid lines) along with those denoted by *p.t.* (dotted lines) obtained in the first order of (degenerate) perturbation theory with respect to $U$ and $V$ (see Sec. IV). As revealed by the comparison of the curves presented in the aforementioned figures, although qualitatively correct, the *p.t.* approximation rapidly worsens with increasing $d$, indicating stronger correlations that cannot be pertubatively accounted for.

As already noted in Sec. V B, with increasing $d$ and concomitant fast reduction of tunneling, there is an overall tendency of diminishing energy separations, with the states becoming agglomerated in narrow energy windows. The failure of the perturbation theory is one manifestation of this fact. Another, yet more important manifestation is the appearance of avoided crossings. Three avoided crossings are visible in

Figs. 6(c), 6(d), 6(g), and 6(h) for five electrons over six QDs: two involving three states—($E^4_{2g}$, $E^5_{2g}$, $E^6_{2g}$) and ($E^3_{2g}$, $E^4_{2g}$, $E^5_{2g}$) at $d \approx 1.555$ and $d \approx 1.685$, respectively—and one with the participation of the pair of states $E^1_{2g}$ and $E^2_{2g}$ at $d \approx 1.765$.

For five electrons on ten QDs (Fig. 7), there is an avoided crossing at $d \simeq 1.795$, which involves the pair $A^1_{1g}$ and $A^2_{1g}$, and another at $d \approx 1.765$ between the pair $E^1_{2g}$ and $E^2_{2g}$. Counterintuitively, for five electrons on ten QDs there are not so many avoided crossings involving $E_{2g}$ states as for five electrons on six QDs. The reason why there are less in the case of ten QDs is similar to that encountered in the analysis of the group of second excitations: the role of certain optically active $E_{2g}$ excitations in the case of six QDs is replaced by certain optically *inactive* $E_{4g}$ excitations.

### B. Case of seven electrons on ten quantum dots

For seven electrons on ten QDs, the ground state is a spin doublet $^2E_{2g}$ state. Because in $D_{10h}$, $\boldsymbol{\mu}|G\rangle \rightarrow E_{1u} \otimes E_{2g} = E_{1u} \oplus E_{3u}$, only eigenstates with spatial symmetries $E_{1u}$ and $E_{3u}$ contribute to absorption. The first group of MO optically active degenerate excitations (excitation energy $t_0$) comprises one $E_{3u}$ and two $E_{1u}$ states. They result from the excitation of one of the four electrons completely occupying the $e_{1u}$ MOs into one empty $e_{2g}$ MO. The second group of MO optically active excitations (excitation energy $1.236t_0$) merely consists of one $E_{3u}$ state. It results from the excitation of the single electron occupying one of the degenerate $e_{2g}$ MOs into one of the degenerate empty $e_{3u}$ MOs.

The results obtained by exact numerical diagonalization are collected in Fig. 8. The lowest optically active excitation possesses $E_{1u}$ symmetry for small $d$, which changes to $E_{3u}$ symmetry beyond $d \simeq 1.1917$. With increasing $d$, correlations split more and more the two $E_{1u}$ states originating from the degenerate group of lowest MO $E_{1u}$ excitations, while higher $E_{1u}$ states come closer in energy to the second excitation. Consequently, a series of avoided crossings can be seen for this symmetry, at $d \simeq 1.59$, $d \simeq 1.81$, and $d \simeq 1.96$, the second with participation of three states. For $E_{3u}$ symmetry, an avoided crossing involving three states is also visible in Fig. 8 around the value $d \simeq 1.71$. Interestingly, at larger $d$ values, not only the energies of the relevant excitations for each symmetry ($E_{1u}$ and $E_{3u}$) become close to each other but also their intensities [see Figs. 8(b) and 8(c)].

### C. Case of nine electrons on ten quantum dots

Similar to the above case of seven electrons on ten QDs, for nine electrons on ten QDs, the ground state is a spin doublet $^2E_{2g}$ state. However, differences exist concerning the first and second excitations in the two cases.

In the present case, the highest occupied MO is an $e_{2g}$. Out of the four single-particle $e_{2g}$ states, three are occupied and one is empty. The lowest MO excitation amounts to the excitation of one electron from the MO below it, $e_{1u}$, into the only empty $e_{2g}$ MO (excitation energy $t_0$), and this yields a $^2E_{1u}$ state. The second MO excitation is the rise of one of the three electrons from the $e_{2g}$ MOs into the empty $e_{3u}$ MOs. This leads to the second group of optically active excitations

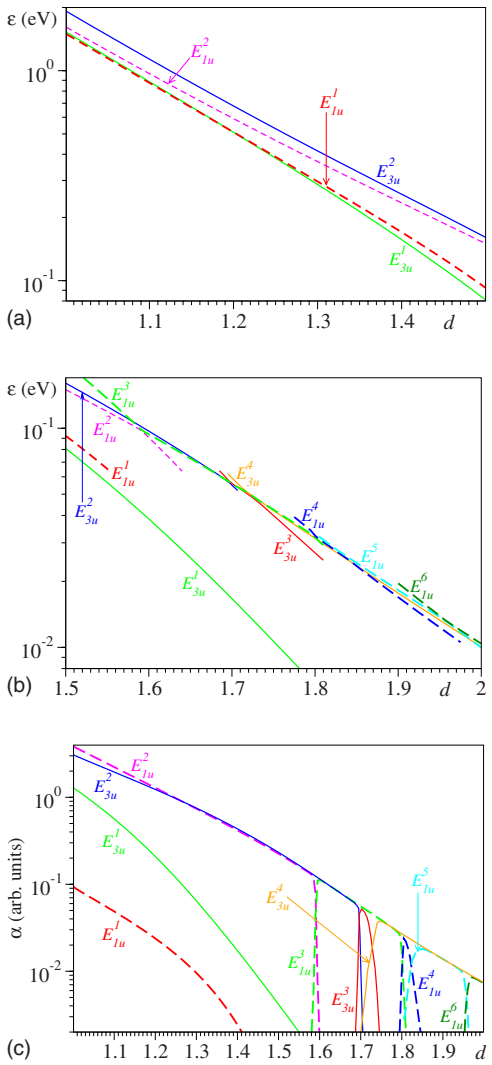


FIG. 8. (Color online) Exact results for [(a) and (b)] energies and (c) spectral intensities of optical absorption for seven electrons on ten QDs in the ground ($E_{2g}$) state. The superscripts indicate the energy ordering of the excited states with a significant spectral intensity.

(excitation energy $1.236t_0$) comprising one $E_{1u}$ and three $E_{3u}$ states.

The exact results for this case, which are presented in Fig. 9, indicate effects of electron correlations similar to the cases exposed in Secs. VI A and VI B: splittings of degenerate MO optical transitions and avoided crossings. One should emphasize that the phenomenon of avoided crossing is more frequently encountered than in the preceding cases. Noteworthy is the sequence of four dense avoided crossings for $E_{3u}$ symmetry, two of them involving three states [see Figs. 9(b) and 9(c)].

### D. Cases of four and eight electrons on ten quantum dots

In both cases of four and eight electrons on ten QDs, two electrons occupy two out of the four single-particle states available in the highest partially occupied MO ($e_{1u}$ and $e_{2g}$, respectively). Accordingly, the ground state is sixfold degen-

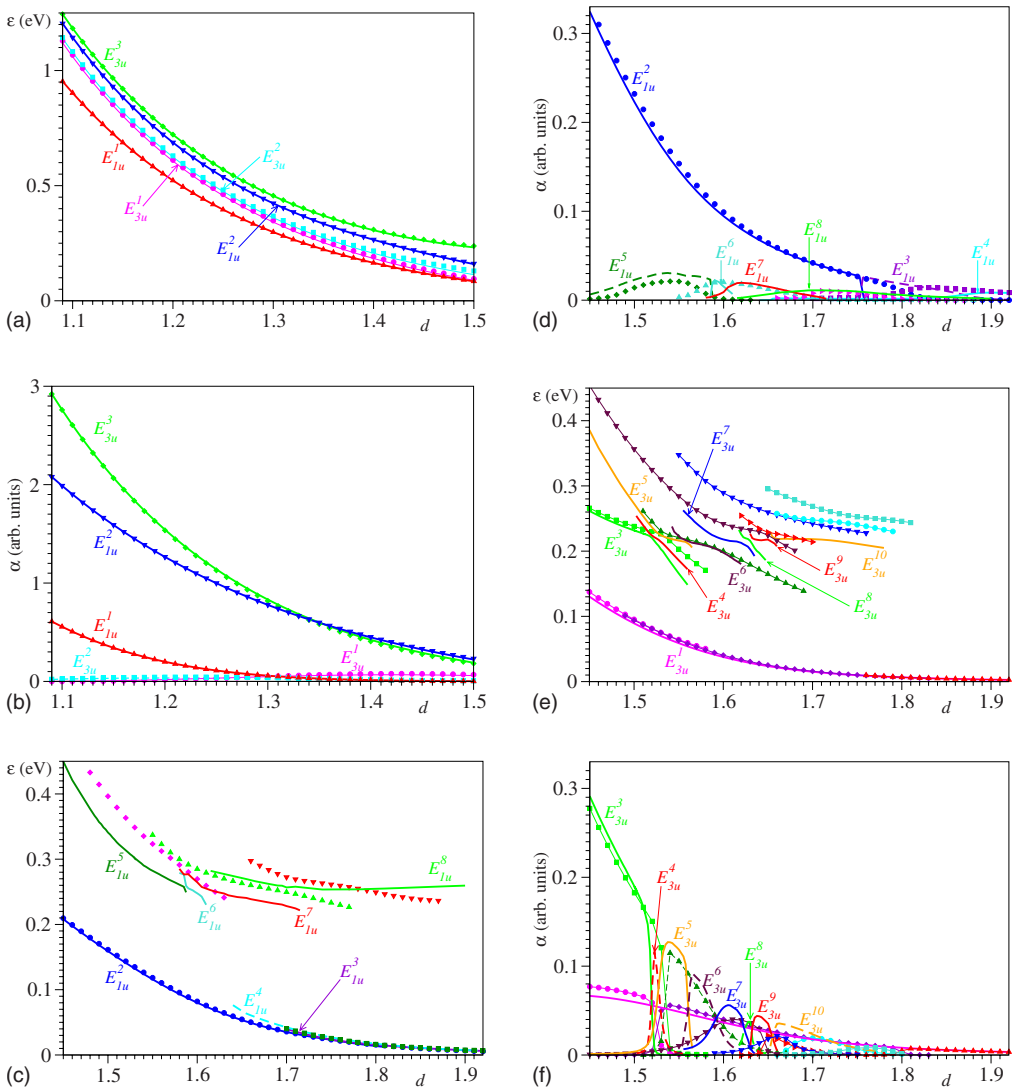


FIG. 9. (Color online) Results for optical absorption of nine electrons on ten QDs obtained exactly (solid lines) and by the *ph* method (see Sec. VII). The latter are depicted by points [for clarity, in (e) and (f), they are joined by the thin lines]. The superscript indicates the energy ordering of the exact excited states with a significant spectral intensity.

erate in the MO picture. The group of these six degenerate states comprises ${}^3A_{2g}$, ${}^1A_{1g}$, and ${}^1E_{2g}$ states for four electrons, and ${}^3A_{2g}$, ${}^1A_{1g}$, and ${}^1E_{4g}$ states for eight electrons. In the range of $d$ shown in Fig. 10, wherein the exact results are collected, the exact ground state is a triplet state ${}^3A_{2g}$, which lies slightly below the other nearly degenerate singlet states. Thus, we are dealing here with nanosystems satisfying the Hund rule, a situation we also encountered for four electrons on six-QD nanorings.

The selection rule in these cases, $\boldsymbol{\mu}|G\rangle \rightarrow E_{1u} \otimes A_{2g} = E_{1u}$, is simpler than in the other cases of open shells discussed above. The optical absorption spectra are also simpler than in those cases. As shown in Fig. 10, they consist of two lines only, and no avoided crossing is present.

## VII. VERY USEFUL APPROXIMATE METHOD: DRESSED PARTICLE-HOLE EXCITATIONS

Even more than the figures presented in Secs. V and VI, the eye-catching aspect from inspecting the curves of the preceding section is the intriguingly extreme simplicity of optical spectra, which is an unexpected fact in view of the strong electron correlations. The detailed analysis reveals that, apart from the splitting of the degenerate transitions, the number of optical signals with a significant intensity coincides with that expected within the MO description.

This feature bears much resemblance with the basic idea of the Landau theory,[36] which postulates a one-to-one map between the low-energy excitations, which are close to the Fermi level, of interacting and noninteracting electron systems. Because of the strong correlations, it makes little sense to attempt to construct approximate excited states by using configurations obtained by acting on the *noninteracting* ground state with the operators of (HOMO-LUMO) particle-hole pairs $\Sigma_\sigma c^\dagger_{p_l,\sigma} c_{p_h,\sigma}$ ($|p_l - p_h| = 1$) that are closest to the Fermi level, i.e., either $p_l$ corresponds to a completely empty MO or $p_h$ to a completely occupied MO. Unless $d$ is very small, this approximation turns out to be indeed very poor. However, in view of the observation of the small number of

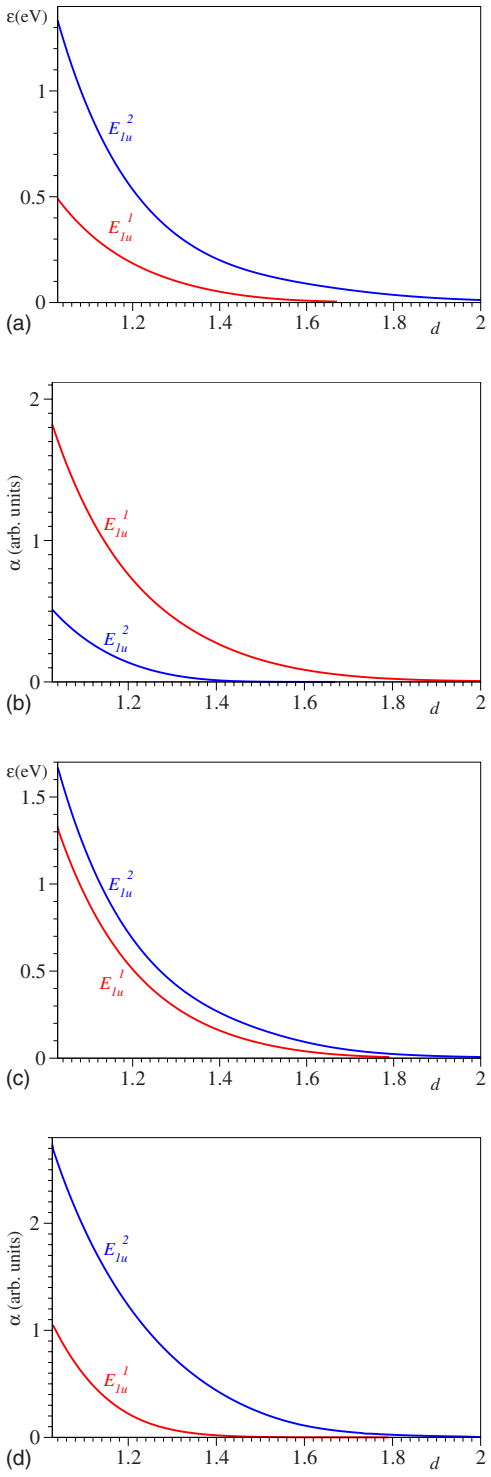


FIG. 10. (Color online) Exact results for energies and spectral intensities of optical absorption for four (upper panels) and eight electrons (lower panels) on ten QDs in the triplet ground ($^3A_{3g}$) state. The superscripts indicate the energy ordering of the excited states with a significant spectral intensity.

optical signals, it looks meaningful to use instead the *interacting* ground state. This approximation, which we denote by *hl-ph*, qualitatively agrees with the exact results, in the sense that it predicts the correct number of significant spectral lines. Unfortunately, for larger $d$, where electron correlations are strong, the quantitative agreement is reasonably good only for half-filling. The latter aspect can be seen by inspecting the *hl-ph* results for half-filling, which are shown together with the exact results in Figs. 3 and 4.

One can extend this idea and consider not only HOMO-LUMO but all dressed particle-hole excitations $\{|p\rangle\}$,

$$\mathcal{O}_p = \sum_\sigma c^\dagger_{p,\sigma} c_{p\pm1,\sigma},$$

$$|p\rangle \equiv \mathcal{O}_p|G\rangle. \tag{6}$$

The operators $\mathcal{O}_p$ are useful because they possess the symmetry $E_{1u}$ of the dipole operator and generate, when applied on the interacting ground state $|G\rangle$, approximative eigenstates with correct spin and spatial symmetry. We have also numerically diagonalized Hamiltonian (1) in the truncated configuration space spanned by these dressed particle-hole excitations. In this way, we have found that all bright transitions can be accurately described. Compare the exact curves to those denoted by *ph* computed by means of this method in Figs. 3–7 and 9. To better see that this approximation provides a good description of the states with a significant spectral intensity (the so-called bright diabatic states), the approximate *ph* curves for energy in Figs. 5(c) and 6(g) have been artificially slightly displaced. The only exact result that cannot be explained by this approach is the avoided crossing, which is less important for the pragmatic purpose of reproducing the spectra.

One should note that this method brings a substantial simplification by drastically reducing the number of configurations used in numerical diagonalization as compared to the total dimension of the Hilbert space of the many-body system. The dimension of the Hamiltonian matrix to be diagonalized is $\sim N$, while that for the exact result is $\sim(2N/N_e)$.

## VIII. OPTICAL GAP VERSUS CHARGE GAP

The charge gap $\Delta$ is a useful quantity to assess whether a many-body system behaves as a Luttinger liquid or not. It is defined as the difference between the chemical potentials $\mu^\pm$ for adding and removing an electron to/from the system, $\Delta = \mu^+ - \mu^-$.[37] The latter are expressed in terms of the ground state energies $E_G$ of the systems with $N_e$ and $N_e \pm 1$ electrons, $\mu^+ = E_G(N_e+1,N) - E_G(N_e,N)$ and $\mu^- = E_G(N_e,N) - E_G(N_e-1,N)$. From the study of infinite chains, it is known that the charge gap of the Hubbard model ($V=0$) is finite at half-filling (Mott–Hubbard gap) and vanishes away from half-filling (see, e.g., Refs. 34 and 35). Accordingly, the system is a Mott insulator or metal, respectively. For finite Hubbard systems, one can expect to observe precursor effects of this behavior in the strong coupling limit $U/t_0 \gg 1$, in which the interaction between sites via tunneling plays only a secondary role and, therefore, the number of sites is not important.

As obvious from their definition, although related from intuitive physical considerations, the charge gap $\Delta$ and the optical gap $\varepsilon$ are not identical. Therefore, it would be interesting to comparatively inspect curves for optical gap and charge gap and to see whether they behave similarly.

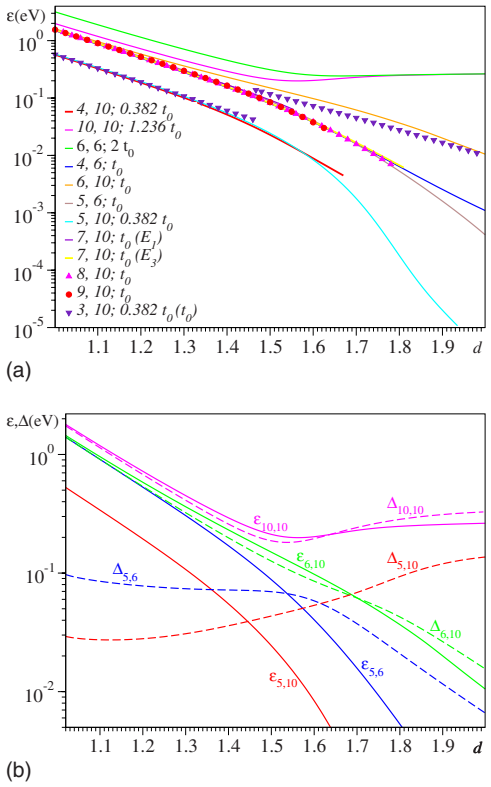


FIG. 11. (Color online) (a) Optical gap $\varepsilon$ for various numbers of electrons ($N_e$) and QDs ($N$). These numbers are indicated in the legend along with the gap value for free electrons. In addition, because the lowest optically active excitation changes the symmetry for seven electrons on ten QDs, its symmetry is also given in parentheses. For three electrons on ten QDs, the ground state switches beyond $d=1.47$ from doublet ($S=1/2$) to quartet ($S=3/2$), and the free gap of the latter case is also indicated in parentheses. (b) Optical gap $\varepsilon_{N_e,N}$ and charge gap $\Delta_{N_e,N}$ for several values of $N_e$ and $N$. The charge gap for five electrons on ten QDs does not tend to zero as for other cases away from half-filling for physical reasons explained in the main text.

In Fig. 11(a), we have collected the results for the optical gap of the finite nanorings studied here. As visible there and partly anticipated in Sec. V A, the optical gap changes its character at around $d\approx 1.5$. Below this value, it scales as the hopping integral $t_0$ and is basically similar to the band (or HOMO-LUMO) gap because the physics manifestly exhibits a single-particle character. For larger $d$, the optical gap tends to a finite value at half-filling and to zero away from half-filling. That is, it reproduces the strong coupling limit of infinite systems, as expected for the restricted Hubbard model.

As a general characterization, as revealed by some typical curves we choose to present in Fig. 11(b), the two kinds of gaps $\varepsilon$ and $\Delta$ often behave qualitatively similar (see the cases of ten electrons on ten QDs and of six electrons on ten QDs). However, significant quantitative differences between $\varepsilon$ and $\Delta$ exist even for these cases (note the logarithmic scale on ordinate).

More important than such quantitative differences, a qualitative difference can be observed for five electrons on ten QDs, which corresponds to quarter filling. There, unlike the optical gap, the charge gap does not fall off more or less exponentially with increasing $d$ but approaches the value $2V$ (see below). The reason is the following: In the strong coupling limit ($U,V\gg t_0$), by increasing the number of electrons up to quarter filling ($N_e=N/2$, where$N$ is even), in the ground state there are neither doubly occupied sites nor sites consecutively occupied because of the large energy penalty ($U$ or $V$, respectively) and, therefore, $E_G(N_e,N)=\mathcal{O}(t_0)$. By adding an extra electron to a quarter filled band, it will occupy an empty site between two sites already occupied with one electron if (and this is the case for the QDs investigated here) the corresponding energy cost $2V$ is lower than that to be paid for double occupancy $U$. Consequently, $E_G(N/2+1,N)=2V+\mathcal{O}(t_0)$, and this straightforwardly yields a charge gap $\Delta_{N/2,N}=2V+\mathcal{O}(t_0)$ for $U>2V\gg t_0$.

Thus, based on the present numerical results, we claim that in the limit $U>2V\gg t_0$ the optical gap of the infinite extended Hubbard model at quarter filling vanishes, while the charge gap reaches a finite value, which is equal to $2V+\mathcal{O}(t_0)$. Needless to say, the difference between the charge and optical gaps is relevant only for the *extended* Hubbard model and does not exist for the restricted Hubbard model ($V=0$). To the best of our knowledge, we are not aware on a previous work reporting this finding for the extended Hubbard model.

## IX. DISCUSSIONS AND CONCLUSIONS

In the present paper, we have extended the study of Ref. 12 on optical absorption of finite tunable nanorings consisting of metallic QDs by considering in detail cases away from half-filling. By varying the interdot spacing, the nanorings can be driven from a weak to a strong correlation regime, a fact that clearly reflects itself in optical absorption. However, in spite of the (very) strong correlations, their effect on optical absorption is intriguingly simple. It is basically twofold: the splitting of degenerate optical excitations in the MO picture and the occurrence of avoided crossings.

Qualitatively, the splitting of the degenerate MO transitions can be understood already by the perturbation theory. Quantitatively, the latter description is very poor in the strong correlation regime. Avoided crossings in nanorings of the type studied here are not too surprising. The interdot spacing plays the role of a giant symmetric stretching mode in a molecule, and avoided crossings in molecules are well known.[38] What makes the difference in the present case is that numerous avoided crossings often occur with the participation of more than two states. To our knowledge, such a feature has not been reported so far in literature. What favors the occurrence of such avoided crossings is the fact that with increasing $d$ and concomitant rapid reduction of tunneling, numerous states condense into almost degenerate groups, which are well separated by energies on the order of $U$ or $V$ (much larger than $t_0$).

The very small number of spectral lines that possess a significant intensity is quite intriguing in view of the strong correlations and the large numbers of transitions allowed by spin conservation and spatial symmetry. For closed shells, even away from half-filling the absorption signal remains

practically monochromatic. This is a generalization of the particular case of half-filling.[12] In the open-shell cases, a *few* optical signals with a significant intensity are present in the spectrum.

Qualitatively, one can understand the small number of the significant spectral lines within Landau's idea to construct low-lying excitations in an interacting electron system, which is an approximation denoted by *hl-ph* in Sec. VII. Quantitatively, this method turned out to be satisfactory only at half-filling. Fortunately, we have been able to extend this method by applying the operators of particle-hole excitations to the fully interacting ground state. This generalization (see Sec. VII), which is briefly denoted by *ph*, has been found to be very accurate for computing the absorption spectra. It is much less demanding than the exact numerical diagonalization; the only notable effort is to determine the ground state.

The scarcity of the optical spectra in all investigated cases is astonishing. It makes us to believe that the conclusion of Ref. 12 is more general: we ascribe this scarcity to a more general hidden dynamical quasisymmetry of the extended Hubbard model for arbitrary filling. Despite extensive efforts to analyze our numerical data, we are unable to more precisely specify this hidden symmetry. What we can solely do at present is to tentatively speculate on a special type of Landau liquid, which is characterized by a one-to-one map between the *optically active* excitations in interacting and noninteracting electron systems. This would be a counterpart of the traditional Landau liquid, wherein there the low-lying (optically active or not) excitations of interacting electrons are in one-to-one correspondence with those of noninteracting electrons. This speculation is based on our observation that there are *exactly* as many optical transitions are expected within the single-particle picture by considering the degeneracy lifted by interactions.

The fact that we have computed individual spectral lines and not only convoluted optical spectra permits us to directly determine the optical gap (i.e., the lowest absorption frequency). The optical gap nicely reveals the crossover from weak to strong correlation regimes. In the weak correlation regime, it behaves as a HOMO-LUMO (or band) gap, a feature specific for single-particle physics. In the strong correlation regime we found a behavior that singles out the half-filling case from the cases away from half-filling. In this way, the strong coupling limit displays features that are precursor to the behavior of the infinite restricted Hubbard chain (Mott–Hubbard insulator and metal, respectively).

The optical gap has also been compared to the charge gap. The latter has been extensively employed to assess whether the infinite restricted Hubbard chain, which is exactly solvable by Bethe ansatz,[34,35] behaves as a Luttinger liquid or not. In spite of many similarities, we have demonstrated (both numerically and analytically) that for quarter filling in the strong coupling limit, the charge gap tends to the value $2V$ (and this obviously vanishes only for the restricted Hubbard model), while the optical gap rapidly falls down to zero.

Of course, a realistic theory of QD nanorings should include many other concrete aspects not considered in the present work. However, by using parameter values determined in literature for a real case (assembled Ag-QDs), with parameters tunable in wide ranges, we think that the present results are of sufficient interest to motivate further experimental work on metallic QD nanorings. In addition to the presently considered metallic QDs, structures of tunable semiconducting nanorings with equidistant barriers, which are already fabricated,[39–41] could also be of interest.

## ACKNOWLEDGMENTS

The authors acknowledge with thanks the financial support for this work provided by the Deutsche Forschungsgemeinschaft (DFG).

*Also at National Institute for Lasers, Plasma, and Radiation Physics, ISS, POB MG-23, RO 077125 Bucharest, Romania. ioan.baldea@pci.uni-heidelberg.de

[1] C. P. Collier, R. J. Saykally, J. J. Shiang, S. E. Henrichs, and J. R. Heath, Science **277**, 1978 (1997).
[2] J. Heath, C. Knobler, and D. Leff, J. Phys. Chem. B **101**, 189 (1997).
[3] G. Markovich, C. P. Collier, and J. R. Heath, Phys. Rev. Lett. **80**, 3807 (1998).
[4] J. Shiang, J. Heath, C. Collier, and R. Saykally, J. Phys. Chem. B **102**, 3425 (1998).
[5] G. Medeiros-Ribeiro, D. A. A. Ohlberg, R. S. Williams, and J. R. Heath, Phys. Rev. B **59**, 1633 (1999).
[6] S. Henrichs, C. Collier, R. Saykally, Y. Shen, and J. Heath, J. Am. Chem. Soc. **122**, 4077 (2000).
[7] J. Sampaio, K. Beverly, and J. Heath, J. Phys. Chem. B **105**, 8797 (2001).
[8] K. Beverly, J. Sampaio, and J. Heath, J. Phys. Chem. B **106**, 2131 (2002).
[9] M. A. Kastner, Phys. Today **46** (1), 24 (1993).
[10] A. Kawaharazuka, T. Saku, Y. Hirayama, and Y. Horikoshi, J. Appl. Phys. **87**, 952 (2000).
[11] H. Kuzmany, *Solid-State Spectroscopy* (Springer, Berlin, 1998).
[12] I. Bâldea and L. S. Cederbaum, Phys. Rev. B **75**, 125323 (2007).
[13] F. Remacle and R. Levine, J. Am. Chem. Soc. **122**, 4084 (2000).
[14] I. Bâldea, A. K. Gupta, L. S. Cederbaum, and N. Moiseyev, Phys. Rev. B **69**, 245311 (2004).
[15] I. Bâldea, H. Köppel, and L. S. Cederbaum, Phys. Rev. B **69**, 075307 (2004).
[16] F. Remacle, C. P. Collier, J. R. Heath, and R. D. Levine, Chem. Phys. Lett. **291**, 453 (1998).
[17] F. Remacle, C. P. Collier, G. Markovich, J. R. Heath, U. Banin, and R. D. Levine, J. Phys. Chem. B **102**, 7727 (1998).
[18] F. Remacle and R. Levine, J. Phys. Chem. A **104**, 10435 (2000).
[19] F. Remacle, J. Phys. Chem. A **104**, 4739 (2000).
[20] F. Remacle and R. Levine, J. Phys. Chem. B **105**, 2153 (2001).
[21] F. Remacle, K. Beverly, J. Heath, and R. Levine, J. Phys. Chem. B **106**, 4116 (2002).
[22] I. Bâldea and L. S. Cederbaum, Phys. Rev. Lett. **89**, 133003 (2002).

[23] H. Köppel, W. Domcke, and L. S. Cederbaum, Adv. Chem. Phys. **57**, 59 (1984).
[24] I. Bâldea, H. Köppel, and L. S. Cederbaum, Phys. Rev. B **55**, 1481 (1997).
[25] D. Bullet, R. Haydock, V. Heine, and M. J. Kelly, in *Solid State Physics*, edited by H. Erhenreich, F. Seitz, and D. Turnbull (Academic, New York, 1980).
[26] P. Fulde, in *Electron Correlations in Molecules and Solids*, Springer Series in Solid-State Sciences Vol. 100 (Springer-Verlag, Berlin, 1991).
[27] E. Dagotto, Rev. Mod. Phys. **66**, 763 (1994).
[28] L. Salem, *The Molecular Orbital Theory of Conjugated Systems* (Benjamin, New York, 1966).
[29] I. Bâldea, H. Köppel, and L. S. Cederbaum, Phys. Rev. B **60**, 6646 (1999).
[30] I. Bâldea, H. Köppel, and L. S. Cederbaum, J. Phys. Soc. Jpn. **68**, 1954 (1999).
[31] An important issue for infinite systems is whether the momentum distribution $n_p$ exhibits or not a jump at $p=k_F$, i.e., whether the interacting electron system behaves as a Landau or Luttinger liquid. We shall not consider the extrapolation of $n_{p_F-\pi/N} - n_{p_F+\pi/N}$ to infinite $N$ since our interest here is in finite nanorings.
[32] A. L. Fetter and J. D. Walecka, *Quantum Theory of Many Particle Systems* (McGraw-Hill, New York, 1971).
[33] A further restriction in the half-filling case comes from the particle-hole symmetry, which further reduces the number of $E_{1u}$ states that may contribute to 32 ($E_{1u}^{-}$ states, see Ref. 14).
[34] N. Andrei, in *Integrable Models in Condensed Matter Physics*, Series on Modern Condensed Matter Physics, Lecture Notes of ICTP Summer Course Vol. 6, edited by S. Lundquist, G. Morandi, and Y. Lu (World Scientific, Singapore, 1992), p. 458.
[35] N. Andrei, arXiv:cond-mat/9408101 (unpublished).
[36] D. Pines, *The Many-Body Problem*, Frontier in Physics (Benjamin, New York, 1962).
[37] E. H. Lieb and F. Y. Wu, Phys. Rev. Lett. **20**, 1445 (1968).
[38] W. T. A. M. Van der Lugt and L. J. Oosterhoff, J. Am. Chem. Soc. **91**, 6042 (1969).
[39] A. Fuhrer, S. Luscher, T. Ihn, T. Heinzel, K. Ensslin, W. Wegscheider, and M. Bichler, Nature (London) **413**, 822 (2001).
[40] D. Granados and J. M. García, Appl. Phys. Lett. **82**, 2401 (2003).
[41] X. Y. Kong, Y. Ding, R. Yang, and Z. L. Wang, Science **303**, 1348 (2004).